CONF-830301--12

DE83 009860

DEVELOPMENT OF A GENERALIZED CORRELATION FOR PHASE-VELOCITY MEASUREMENTS OBTAINED FROM IMPEDANCE-PROBE PAIRS IN TWO-PHASE FLOW SYSTEMS*

C. T. Hsu†
E. G. Keshock†
R. N. McGill§

ABSTRACT

A flag type electrical impedance probe has been developed at the Oak Ridge National Laboratory (ORNL) to measure liquid- and vapor-phase velocities in steam-water mixtures flowing through rod bundles. Measurements are made by utilizing the probes in pairs, installed in line, parallel to the flow direction, and extending out into the flow channel. Details of the probe design are presented elsewhere (1).

Velocity indications are obtained by correlating the signals that are produced by the sensors as a result of the random fluctuations of the two-phase flow in the channel. Initial studies by McGill have yielded velocity correlations in terms of the void fraction and a quantity v_{noise} generated from a Fourier transform analysis of the flag probe signals (2). The correlations were successful in terms of reproducing corresponding liquid and vapor velocities as calculated by the separated flow model (±30%). However, these correlations do not work well when used with air-water data. Furthermore, their general applicability may be questioned since they were essentially derived from test data alone.

The present study addresses both of the foregoing difficulties by examining from a fundamental point of view the two-phase flow system which the impedance probes typically operate in. Specifically, the governing equations (continuity, momentum, energy) were formulated for both air-water and steam-water systems, and then subjected to a scaling analysis. The scaling analysis yielded the appropriate dimensionless parameters of significance in both kinds of systems. Additionally, with the aid of experimental data obtained at ORNL, those parameters of significant magnitude were established. As a result, a generalized correlation was developed for liquid and vapor phase velocities that makes it possible to employ the impedance probe velocity measurement technique in a wide variety of test configurations and fluid combinations.

NOMENCLATURE

A	bundle free flow area, cross-sectional area
G	gravitational acceleration
H	latent heat of vaporization
h	enthalpy
L	axial length
m	mass flow rate
P	pressure
P(0)	pressure at middle of test section
p	perimeter
q''	heat flux
t	time
V	axial velocity
x	mass vapor quality
Z	axial coordinate
α	void fraction
ρ	density
τ	shear stress
Γ	rate of vapor generation per unit volume
σ	liquid surface tension
σ_{ref}	water surface tension at 24°C

SUBSCRIPTS

f	liquid phase
g	vapor phase
i	interface between two phases
w	wall
o	reference value

*Research sponsored by Division of Reactor Safety Research, U.S. Nuclear Regulatory Commission under Interagency Agreements DOE 40-551-75 and 40-552-75 with the U.S. Department of Energy under contract W-7405-eng-26 with the Union Carbide Corporation.

†Graduate Research Assistant, University of Tennessee, Knoxville, TN
‡Professor, Mechanical and Aerospace Engineering Department, University of Tennessee, Knoxville, TN
§Research Engineer, Oak Ridge National Laboratory, Oak Ridge, TN

INTRODUCTION

Local measurements of thermohydraulic phenomena in light water reactor loss-of-coolant experiments are difficult to make because of several factors. In addition to the usual problems of measurements in transient two-phase flows, the environmental conditions severely limit the types of sensors and instruments which can be used. The series of pressurized water reactor (PWR) reflood simulation experiments (International 2D/3D Program for Reflood Studies) conducted by Germany, Japan, and the United States is a good example of the difficult problems which must be solved. In these experiments, various portions of a (PWR) primary steam system are simulated. A reflood transient is studied by injecting cooling water into a reactor vessel, which contains electrically heated rods to simulate the nuclear core. Typical conditions of exposure for sensors include steam temperatures as high as 900°C and a rapid, violent quench by the cooling water. The need to measure void fraction and fluid velocities inside the test vessel led to consideration of electrical impedance sensors for this purpose.

The use of impedance probes for void fraction measurement has been reported by Del Tin and Negrini (3) and many other investigators over the past several years. The signal processing techniques for determining transit times between two sensors by cross-correlation are also well established. Although many potential problems were obvious, it seemed that impedance probes gave a reasonable chance of obtaining these measurements. Therefore an effort was undertaken to develop sensors for measuring void fraction and liquid and vapor phase velocities. The materials, fabrication, and electrical measurement problems have been presented in other publications (4,5). This paper will deal with the analysis and interpretation of impedance signals to obtain fluid (liquid and vapor) velocities.

MEASUREMENT OF FLUID IMPEDANCE

The type of impedance probe employed in the present study consists of a pair of electrodes mounted in a sealed ceramic insulator as illustrated in Figs. 1 and 2. The electrodes are exposed to the fluid so that the electrode-to-electrode current is modulated by the impedance of the fluid mixture in their vicinity.

The void fraction is determined from the value of mixture impedance relative to that of the separate phases. Details of the method are presented in Ref. (1). The velocity is determined by correlating the signals from the two sensors produced by random fluctuations in the flow as it moves along the subchannel. Random signal analysis methods for estimating propagation delays are well established (6).

THE TEST FACILITY

All of the results reported herein were obtained by using the Advanced Instrumentation for Reflood

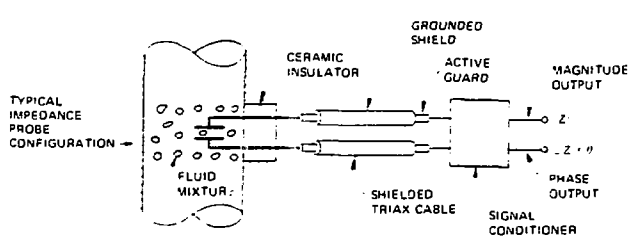

Fig. 1. Illustration of Fluid Impedance Measurement System.

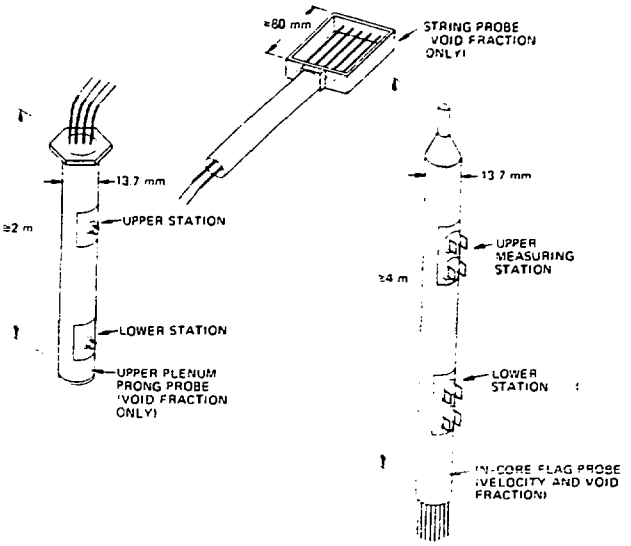

Fig. 2. Impedance Probe Configurations for Reflood Experiments.

Studies (AIRS) test stand. This facility was designed primarily for the purpose of testing prototype designs for in-core impedance probes. Further descriptive details of this test facility are presented in Ref. (7). The test facility is capable of operating as a steam-water or air-water system, with a wide range of both total mass flux and void fractions. For the steam-water tests, data were taken at three pressure conditions, 724, 512, and 306 kPa. For the air-water tests, data were taken at a pressure range of 98 to 147 kPa. The facility is capable of a water flow rate range of 0 to 68 L/min, steam flow rate range of 0 to 0.76 kg/s and an air flow rate range of 0 to 0.28 kg/s. All conditions tested were for steady-state, co-current upflow situations. Void fractions were limited to values greater than 0.5.

Two different configurations of the test facility were used during the course of these experiments. The first was in connection with testing prototype impedance probes for the Primary Cooling Loop (PKL) in West Germany (11). This configuration is shown in Fig. 3. Note that the bundle, even though it is full scale length of a reactor core -- about 4.25 m -- is only a small portion of the total upflow length of the test stand. Also, the mixer section, located below the bundle, gives ample length for the steam and water to mix before the mixture passes through the bundle. Also, notice that the triple-beam gamma densitometer, which is used to determine the void fraction of the mixture, is located on the instrumented spool piece, well above the bundle exit.

The second configuration of the test facility used in this work was as illustrated in Fig. 4. This configuration was for testing prototype impedance probes for the Slab Core Test Facility-1 (SCTF-1) and for the Cylindrical Core Test Facility (CCTF), both in Japan (11). In this case the flag impedance probe design was precisely the same as that for the PKL tests, but the bundle is oriented differently to reflect the fact that the instrument cables will exit the bottom of the pressure vessel in the SCTF-1 and CCTF tests. The only real differences manifested in the test facility because of this change are that (1) there is more distance for mixing of steam and water before entering the

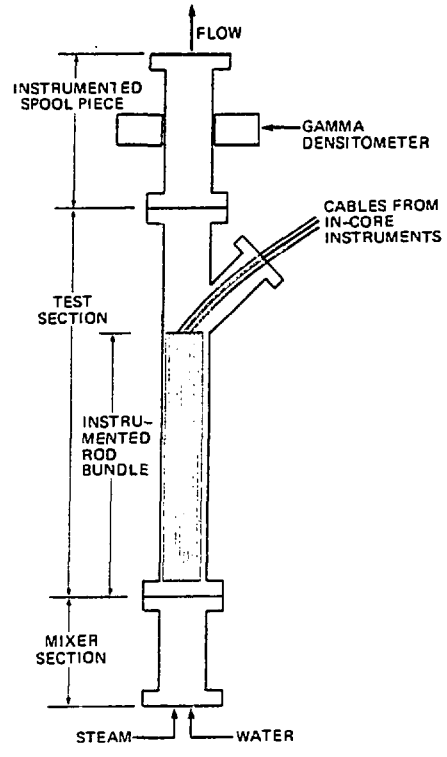

Fig. 3. Test Stand Configuration for PKL Flag Probes.

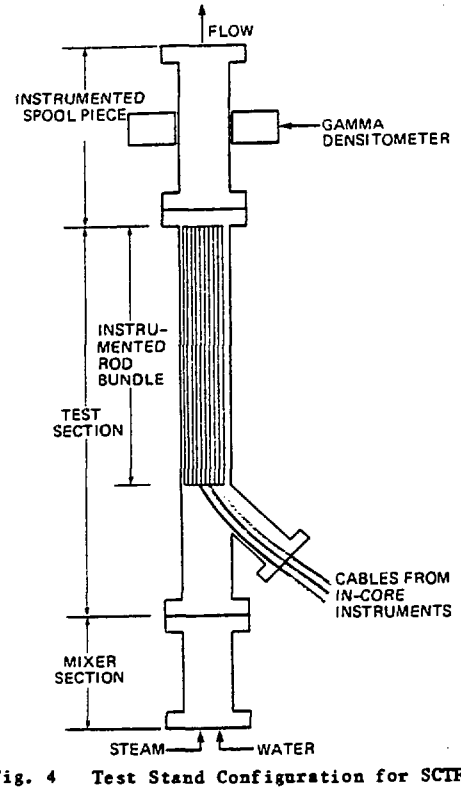

Fig. 4 Test Stand Configuration for SCTF-1 Flag Probes and CCTF Flag Probes.

bundle, and (2) there is less distance after leaving the bundle before the mixture enters the instrumented spool piece.

In all of the test series the procedures, in terms of setting test points and taking data, were the same. Generally, a given water flow rate was set while the steam flow was varied to yield a range of void fractions at a given water flow rate. Then, the water flow rate would be changed to another value and several more steam flow levels would be tested.

From the impedance probes two pieces of information can be obtained on a transient basis, the void fraction, α, and a "transit-time" velocity, V_{noise}. As was mentioned previously, random signal analysis methods, namely the Fast Fourier Transform technique, is applied to the signals from paired impedance probes. In this way a phase difference between the two signals can be determined. The phase difference can be interpreted as a time delay for random flow fluctuations to travel from one probe to its paired probe. In turn, with the distance between the paired probes known, a transit-time velocity can be determined from the time delay. This "transit-time" velocity, called here V_{noise}, is so-named because techniques normally used in noise analysis are used to extract it from the impedance probe signals.

In terms of physical reality, V_{noise} is neither the liquid velocity nor the gas velocity -- generally, it has a value between the two. However, whatever V_{noise} actually is, it is used here, along with the void fraction, to develop correlations that yield the liquid and gas phase velocities in the bundle.

The overall objective in this study is to find phase velocity correlations as follows. Using the void fraction, α, as given by the gamma densitometer and V_{noise} from the impedance probes as independent variables, find accurate relationships that will yield the liquid velocity, V_f, and gas velocity, V_g, just as if they were calculated by the separated flow model equations, which are as follows:

$$V_f = \left(\frac{\dot{m}_f + \dot{m}_g}{A} \right) \frac{1}{\rho_f} \frac{(1 - x)}{(1 - \alpha)}$$

$$V_g = \left(\frac{\dot{m}_f + \dot{m}_g}{A} \right) \frac{1}{\rho_g} \frac{x}{\alpha}$$

The separated flow model was earlier chosen as the standard to which correlations should be compared (8), because it is a model that is straightforward and uses only quantities either measured directly or those calculated from measured quantities (e.g., mass fluxes).

Previous studies by McGill (2) produced empirical correlations for v_f and v_g that were in substantial agreement with values predicted by the separated flow model ($\pm$30%). In those studies the empirical correlations developed were based upon data obtained from the PKL flag probe data. The correlations so developed were then used to successfully predict the fluid velocities in the SCTF tests. However, the correlation(s) developed had different "break" points for the gas and liquid correlations that did not appear to be related to any physical phenomena. Furthermore, when the correlations were applied to data obtained from air-water tests with the SCTF flag probes, the agreement was quite poor. Thus, the desired generality of the correlations did not appear to exist.

Consequently, the foregoing difficulties have been addressed in the present study by examining from a fundamental point of view the two-phase flow system in

which the impedance probes typically would be expected to operate. Specifically, the governing equations of continuity, momentum, and energy were formulated for both air-water and steam-water systems. The equations were then subjected to a systematic scaling analysis (2), from which were obtained the parameters of possible significance in both of the systems. Additionally, however, experimental data obtained from both steam-water and air-water tests at ORNL were used to establish the relative significance of the dimensionless parameters in each system. Those parameters of significance then formed the basis for new correlations which were then applied to a variety of additional test results as a test of their accuracy and generality. The following section describes the development of those correlations.

ANALYSIS AND DEVELOPMENT OF CORRELATIONS

The one-dimensional transient field equations for a separated two-phase flow are as follows:

CONTINUITY

$$\frac{\partial}{\partial t}\left(\alpha_f \rho_f\right) + \frac{\partial}{\partial Z}\left(\alpha_f \rho_f V_f\right) = -\Gamma , \tag{1-a}$$

$$\frac{\partial}{\partial t}\left(\alpha_g \rho_g\right) + \frac{\partial}{\partial Z}\left(\alpha_g \rho_g V_g\right) = \Gamma . \tag{1-b}$$

where $\alpha_f + \alpha_g = 1$.

MOMENTUM

$$\frac{\partial}{\partial t}\left(\alpha_f \rho_f V_f\right) + \frac{\partial}{\partial Z}\left(\alpha_f \rho_f V_f^2\right) = -\frac{\partial(\alpha_f P)}{\partial Z} - \alpha_f \rho_f G - \Gamma V_f + \frac{\tau_i p_i}{A} - \frac{\tau_{wf} p_{wf}}{A} , \tag{2-a}$$

$$\frac{\partial}{\partial t}\left(\alpha_g \rho_g V_g\right) + \frac{\partial}{\partial Z}\left(\alpha_g \rho_g V_g^2\right) = -\frac{\partial(\alpha_g P)}{\partial Z} - \alpha_g \rho_g G + \Gamma V_f - \frac{\tau_i p_i}{A} - \frac{\tau_{wg} p_{wg}}{A} . \tag{2-b}$$

ENERGY

$$\frac{\partial}{\partial t}\left[\alpha_f \rho_f \left(h_f - \frac{P}{\rho_f}\right)\right] + \frac{\partial}{\partial Z}\left(\alpha_f \rho_f V_f h_f\right) = \frac{q_w'' p_{wf}}{A} + \frac{q_i'' p_i}{A} - \Gamma H - P\frac{\partial \alpha_f}{\partial t} , \tag{3-a}$$

$$\frac{\partial}{\partial t}\left[\alpha_g \rho_g \left(h_g - \frac{P}{\rho_g}\right)\right] + \frac{\partial}{\partial Z}\left(\alpha_g \rho_g V_g h_g\right) = \frac{q_w'' p_{wg}}{A} - \frac{q_i'' p_i}{A} + \Gamma H - P\frac{\partial \alpha_g}{\partial t} . \tag{3-b}$$

Only the steady-state equations are considered further, since all test measurements were obtained during steady flow conditions. These equations may be "scaled" in terms of the intrinsic reference variables of the two-phase flow system. This process is a routine mathematical formalism from one perspective; however, the choice of the appropriate (i.e., physically meaningful) reference variables is sometimes not routine or obvious at all. The choice of the appropriate reference variables must sometimes be made, therefore, with the aid of physical information, data, or behavior of the real system being examined. That is, the prior determination of the appropriate reference variables is not always possible or obvious, particularly in complex systems, such as in a two-phase flow in an instrumented rod bundle.

Nevertheless, one must proceed first with scaling the equations with reference variables, denoted by the subscript o. Then one should proceed to establish the magnitudes of these quantities (or more likely, groupings of these quantities) with the aid of experimental information. The scaled equations then become:

CONTINUITY

$$\frac{\partial}{\partial \bar{Z}}\left(\bar{\alpha}_f \bar{\rho}_f \bar{V}_f\right) = \frac{L\Gamma_o}{\alpha_{fo}\rho_{fo}V_{fo}}\left(-\bar{\Gamma}\right) , \tag{4-a}$$

$$\frac{\partial}{\partial \bar{Z}}\left(\bar{\alpha}_g \bar{\rho}_g \bar{V}_g\right) = \frac{L\Gamma_o}{\alpha_{go}\rho_{go}V_{go}}\left(\bar{\Gamma}\right) . \tag{4-b}$$

MOMENTUM

$$\frac{\partial}{\partial \bar{Z}}\left(\bar{\alpha}_f \bar{\rho}_f \bar{V}_f^2\right) = -\frac{\Delta P}{\rho_{fo}V_{fo}^2}\frac{\partial}{\partial \bar{Z}}\left(\bar{\alpha}_f \bar{P}\right) - \frac{P(0)}{\rho_{fo}V_{fo}^2}\left(\frac{\partial \bar{\alpha}_f}{\partial \bar{Z}}\right) - \frac{LG_o}{V_{fo}^2}\left(\bar{\alpha}_f \bar{\rho}_f \bar{G}\right) - \frac{L\Gamma_o}{\alpha_{fo}\rho_{fo}V_{fo}}\left(\bar{\Gamma}\,\bar{V}_f\right) + \frac{L\tau_{io}p_{io}}{\alpha_{fo}\rho_{fo}V_{fo}^2 A_o}\left(\frac{\bar{\tau}_i \bar{p}_i}{\bar{A}}\right) - \frac{L\tau_{wfo}p_{wfo}}{\alpha_{fo}\rho_{fo}V_{fo}^2 A_o}\left(\frac{\bar{\tau}_{wf}\bar{p}_{wf}}{\bar{A}}\right), \tag{5-a}$$

$$\frac{\partial}{\partial \bar{Z}}\left(\bar{\alpha}_g \bar{\rho}_g \bar{V}_g^2\right) = -\frac{\Delta P}{\rho_{go}V_{go}^2}\frac{\partial}{\partial \bar{Z}}\left(\bar{\alpha}_g \bar{P}\right) - \frac{P(0)}{\rho_{go}V_{go}^2}\left(\frac{\partial \bar{\alpha}_g}{\partial \bar{Z}}\right) - \frac{LG_o}{V_{go}^2}\left(\bar{\alpha}_g \bar{\rho}_g \bar{G}\right) + \frac{L\Gamma_o V_{fo}}{\alpha_{go}\rho_{go}V_{go}^2}\left(\bar{\Gamma}\,\bar{V}_f\right) - \frac{L\tau_{io}p_{io}}{\alpha_{go}\rho_{go}V_{go}^2 A_o}\left(\frac{\bar{\tau}_i \bar{p}_i}{\bar{A}}\right) - \frac{L\tau_{wgo}p_{wgo}}{\alpha_{go}\rho_{go}V_{go}^2 A_o}\left(\frac{\bar{\tau}_{wg}\bar{p}_{wg}}{\bar{A}}\right) . \tag{5-b}$$

ENERGY

$$\frac{\partial}{\partial \bar{Z}}\left(\bar{\alpha}_f \bar{\rho}_f \bar{V}_f \bar{h}_f\right) = \frac{Lq_{wo}'' p_{wfo}}{\alpha_{fo}\rho_{fo}V_{fo}h_{fo}A_o}\left(\frac{\bar{q}_w'' \bar{p}_{wf}}{\bar{A}}\right) + \frac{Lq_{io}'' p_{io}}{\alpha_{fo}\rho_{fo}V_{fo}h_{fo}A_o}\left(\frac{\bar{q}_i'' \bar{p}_i}{\bar{A}}\right) - \frac{L\Gamma_o H_o}{\alpha_{fo}\rho_{fo}V_{fo}h_{fo}}\left(\bar{\Gamma}\,\bar{H}\right) , \tag{6-a}$$

$$\frac{\partial}{\partial \bar{Z}}\left(\bar{\alpha}_g \bar{\rho}_g \bar{v}_g \bar{h}_g\right) = \frac{L q''_{wo} p_{wgo}}{\alpha_{go}\rho_{go} V_{go} h_{go} A_o}\left(\frac{\bar{q}''_w \bar{p}_{wg}}{\bar{A}}\right)$$

$$- \frac{L q''_{io} p_{io}}{\alpha_{go}\rho_{go} V_{go} h_{go} A_o}\left(\frac{\bar{q}''_i \bar{p}_i}{\bar{A}}\right) + \frac{L \Gamma_o H_o}{\alpha_{go}\rho_{go} V_{go} h_{go}}(\bar{\Gamma}\ \bar{H}) \quad . \quad (6\text{-b})$$

Details of scaling in two-phase flow systems, together with more generalized equations may be found in Ref. (10), by Ishii. Thus, at this point the basis for establishing similitude in two similar-geometry two-phase flow systems is that all of the respective coefficients in each of the Eqs. (4)-(6) for both systems must be of the same magnitude. However, one would then be faced with the very difficult task of attempting to match numerous groups of parameters to insure such similitude (providing that one has already established the intrinsic reference variables). Furthermore, some of these parameter groupings may in reality be negligibly small compared with others. Scaling with intrinsic reference variables insures that the bracketed terms of Eqs. (4)-(6) are of order unity. Thus, comparing the magnitudes of the groupings of terms preceding each of the bracketed quantities establishes the relative importance of each of the terms in Eqs. (4)-(6). Thus, if only the most significant terms in Eqs. (4)-(6) may be established (with the aid of experimental data, in the present case) the development of a correlation is then possible, hopefully involving only very few dimensionless parameters.

Some simplifications may be made immediately, however, as follows:

1. Since equilibrium conditions probably exist in the tests conducted (Ref. 1), it is assumed that no interfacial exchanges of mass, momentum, and energy are occurring. Therefore, $\Gamma = 0$ and $q''_i = 0$.
2. For adiabatic flows (no rod-bundle or wall heating occurs and the test loop is well insulated), $q''_w = 0$.
3. Flashing due to pressure drop in the test section is assumed to be negligibly small, so that no flow accelerations exist in the upward co-current flow. Accordingly, the void fraction is therefore a constant.

Furthermore, for the high void fractions, high quality test and reflood conditions, it is assumed that an annular type flow pattern exists (in the broad sense that there is no contact between the vapor phase and the solid wall). Thus,

$$\tau_{wgo} = 0$$

The scaled momentum equations, from Eqs. (5-a) and (5-b) then become:

$$\frac{\partial(\bar{\alpha}_f \bar{P})}{\partial \bar{Z}} = - \frac{\rho_{fo} L\ G_o}{\Delta P}\left(\bar{\alpha}_f \bar{\rho}_f \bar{G}\right) + \frac{L\ \tau_{io} p_{io}}{\alpha_{fo}\Delta PA_o}\left(\frac{\bar{\tau}_i \bar{p}_i}{\bar{A}}\right)$$

$$- \frac{L\tau_{wo}\ p_{wo}}{\alpha_{fo}\Delta PA_o}\left(\frac{\bar{\tau}_w \bar{p}_w}{\bar{A}}\right), \quad (7)$$

$$\frac{\partial(\bar{\alpha}_g \bar{P})}{\partial \bar{Z}} = - \frac{\rho_{go} LG_o}{\Delta P}\left(\bar{\alpha}_g \bar{\rho}_g \bar{G}\right) - \frac{L\tau_{io} p_{io}}{\alpha_{go}\Delta PA_o}\left(\frac{\bar{\tau}_i \bar{p}_i}{\bar{A}}\right). \quad (8)$$

Now one may estimate the magnitudes of the terms in these scaled equations by inserting actual test and system data. Numerous data sets have been so utilized to establish the orders of magnitude of the groupings of terms in Eqs. (7)-(8) (11). Only the parameter $(\rho_g LG)/\Delta P$ was found to be negligibly small compared to others. Consequently, the appropriate governing equations (not scaled) are as follows:

$$(1 - \alpha)\frac{dP}{d\bar{Z}} = - (1 - \alpha)\rho_f G + \frac{\tau_i p_i}{A} - \frac{\tau_w p_w}{A}, \quad (9)$$

$$\alpha \frac{dP}{dZ} = - \frac{\tau_i p_i}{A} \quad (10)$$

where $(1 - \alpha) = \alpha_f$ and $\alpha = \alpha_g$.

The appropriate dimensionless parameters are thus indicated to be:

(1) $(\rho_f LG)/(-\Delta P)$ (2) $(L\tau_i p_i)/[-(1 - \alpha)\Delta PA]$

(3) $(L\tau_w p_w)/[-(1 - \alpha)\Delta PA]$ (4) $(L\tau_i p_i)/(-\alpha\Delta PA)$.

The first three of the preceding dimensionless parameters are obtained from the liquid phase scaled equation, Eq. (7), while the fourth is obtained from Eq. (8). It is to be noted that the second and third parameters are essentially equivalent for annular flows (high void fraction), which are precisely the conditions for most of the tests conducted as part of this study. The fourth parameter, $(L\tau_i p_i)/(-\alpha\Delta PA)$, is essentially constant and thus would not be a significant scaling parameter. The terms $\tau_i p_i/A$ and $\tau_w p_w/A$ may be solved for from Eqs. (9) and (10), such that the second of the above dimensionless parameters is of the form $\alpha/(1 - \alpha)$. Thus the appropriate correlating dimensionless parameters indicated by the scaled governing equations (in combination with evaluation of the relative magnitudes of all of the dimensionless parameters of the scaled governing equations, via experimental measurements), are simply $\rho_f LG/(-\Delta P)$ and $\alpha/(1 - \alpha)$. However, since the liquid and vapor velocities are inherently related to the quantity V_{noise} by virtue of the measurement technique employed, the additional relevant parameters are the ratios V_f/V_{noise} and V_g/V_{noise}. Finally, in order that data for differing fluid systems at different pressure (temperature) levels be "brought together" with a single correlation, it appears an additional term, σ/σ_{ref} should also be included. The choice of this parameter is a reflection that flow characteristics are affected by differing fluid surface tensions at different temperature levels. The choice of the dimensionless parameter σ/σ_{ref} is one that is made as a result of experience and judgement, rather than being a result of any formalized scaling procedure.

In summary, the correlating parameters chosen here for the liquid phase velocity are as follows:

$$\rho_f LG/(-\Delta P) \quad ; \quad \alpha/(1 - \alpha)$$

$$V_f/V_{noise} \quad ; \quad \sigma/\sigma_{ref}$$

For the vapor phase velocity, the only dimensionless parameter obtained from the scaled vapor phase equation is $(L\tau_i p_i)/(-\alpha\Delta PA)$, which, as discussed earlier, is essentially a constant value and therefore inappropriate as a scaling parameter. Consequently quantity $\alpha/(1 - \alpha)$, which reflects the magnitude of the interfacial shear parameter for the liquid phase, is chosen again for the vapor phase correlation. Additionally, the parameter $\rho_f V_f^2/(-\Delta P)$, obtained from the acceleration

term, Eq. (5-a), is chosen. This parameter is small in relative magnitude in the liquid phase scaled equation but is included here since the vapor phase velocity is influenced by the liquid phase velocity to some extent when flashing occurs in the system (due to pressure drop). Thus, the correlating parameters chosen for the vapor phase are as follows:

$$\alpha/(1-\alpha) \quad ; \quad \rho_f V_f^2/(-\Delta P)$$

$$V_g/V_{noise}$$

Having so obtained the appropriate scaling parameters, the following correlations were developed, based upon data from the CCTF 306 KPa tests:

$$V_f/V_{noise} = 0.2567\left(\frac{\rho_f LG}{-\Delta P}\right)^{-0.2031}\left(\frac{\alpha}{1-\alpha}\right)^{0.6565}\left(\frac{\sigma}{\sigma_{ref}}\right)^{-0.69}, \tag{11}$$

$$V_g/V_{noise} = 0.1778\left(\frac{\rho_f V_f^2}{-\Delta P}\right)^{-0.855}\left(\frac{\alpha}{1-\alpha}\right)^{1.407}. \tag{12}$$

The correlation results are illustrated in Figs. 5-7, for liquid velocities, and Figs. 8-10 for vapor phase velocities. The data spread is seen to be consistently within ±25% for v_f and ±30% for v_g,* except at low v_f and v_g values, where it is likely that an annular flow pattern does not exist. The correlations, furthermore, are quite successful for either steam-water or air-water systems, constituting a considerable improvement upon the earlier obtained empirical correlations presented in Ref. (2).

*See Appendix I for uncertainty analysis of v_f and v_g.

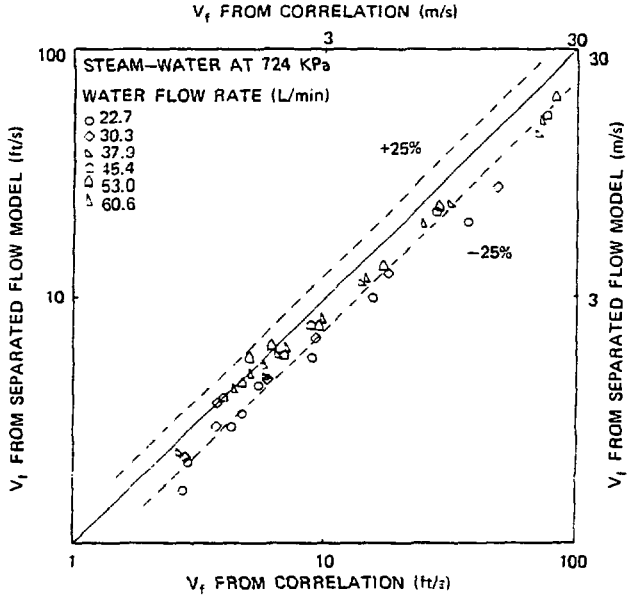

Fig. 5. PKL Liquid Velocity Correlation Results.

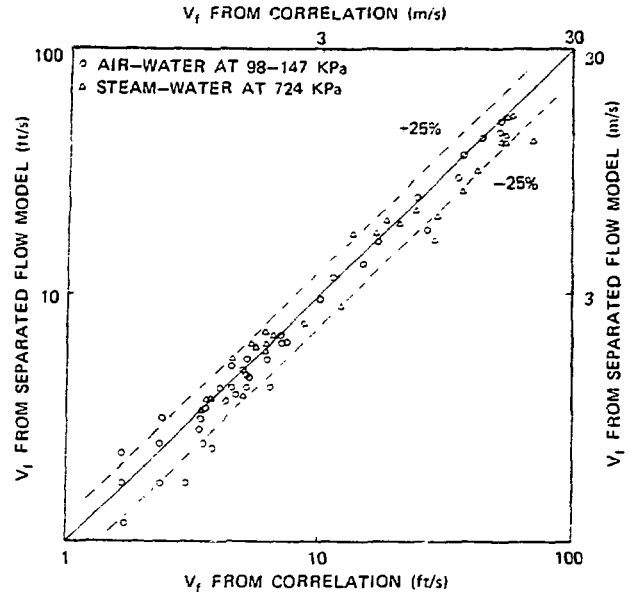

Fig. 6. SCTF-1 Liquid Velocity Correlation Results.

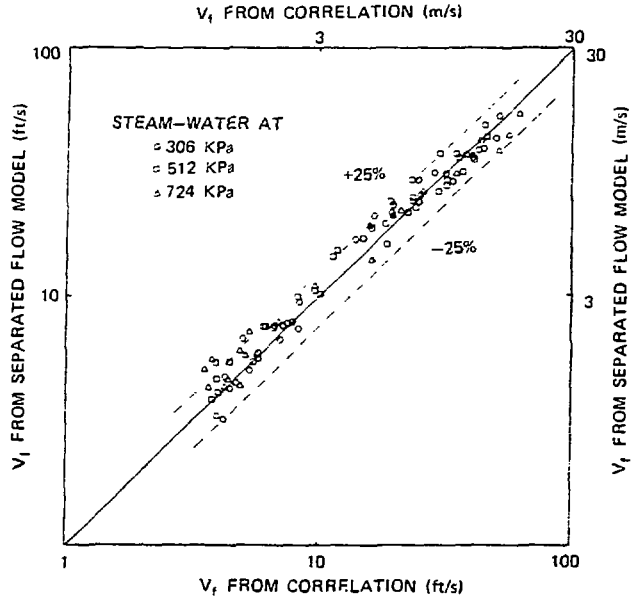

Fig. 7. CCTF Liquid Velocity Correlation Results.

In Figs. 8-10 for vapor phase velocities, the correlation represented by Eq. (12) appears to be inadequate at lower velocities, as reflected by several data points falling well outside the ±30% band. It was established that for such lower vapor velocities these points were not in the annular flow region as predicted by the Hewitt-Roberts flow regime map (12). Since the correlations developed in Eqs. (11) and (12) are based upon an annular type flow, it was reasonable to develop another correlating expression applicable at the lower

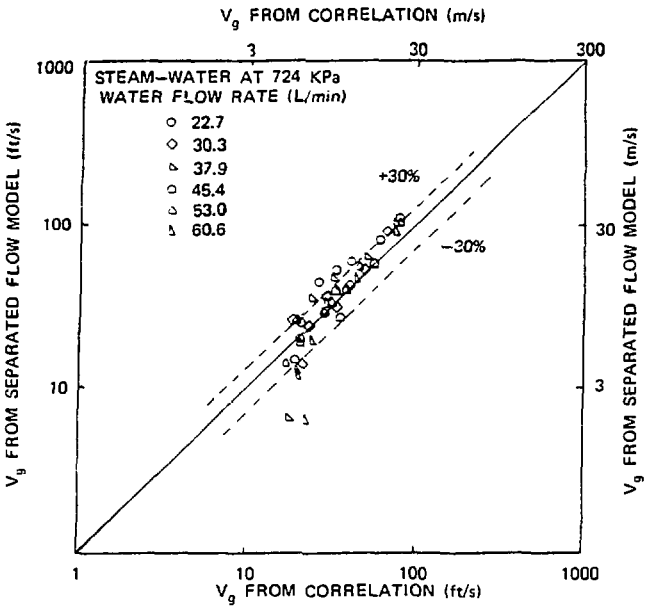

Fig. 8. PKL Vapor Velocity Correlation Results.

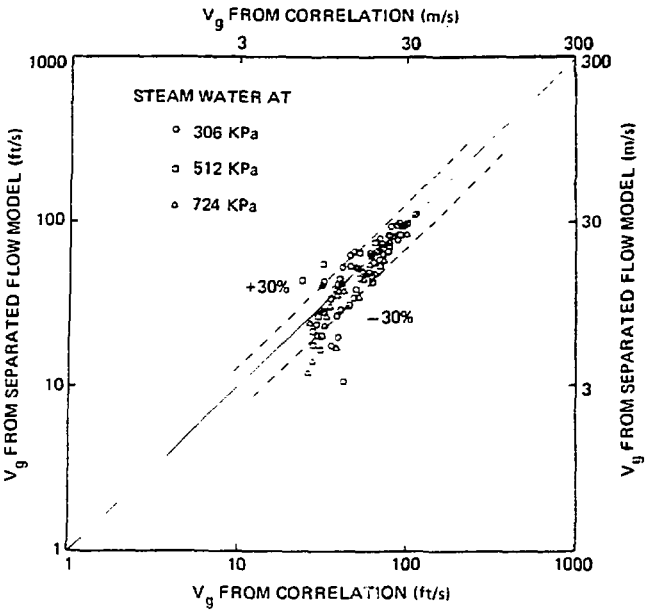

Fig. 10. CCTF Vapor Velocity Correlation Results.

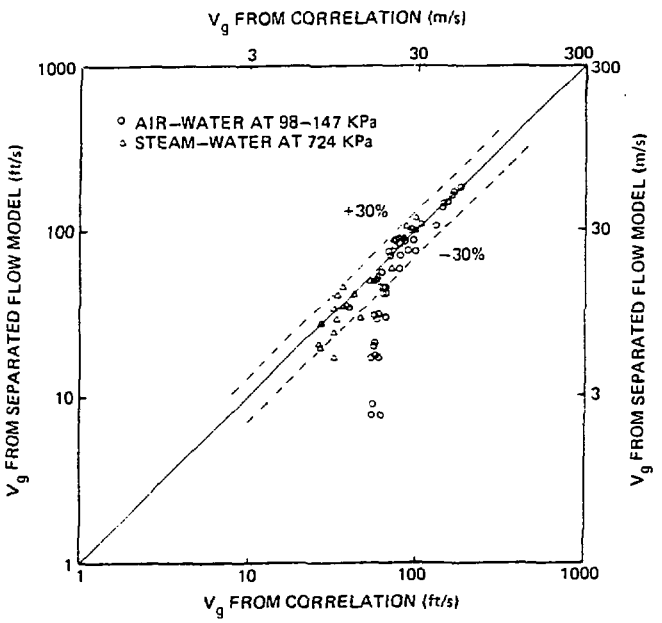

Fig. 9. SCTF-1 Vapor Velocity Correlation Results.

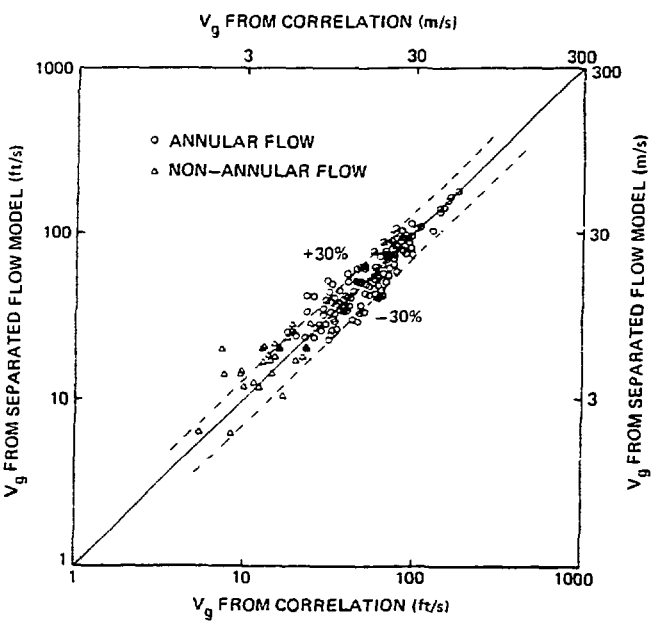

Fig. 11. PKL, SCTF-1, and CCTF Vapor Velocity Correlation Results Using Two Equations.

vapor phase velocities, given by the following expression:

$$V_g/V_{noise} = 0.10705\left(\frac{\rho_f V_f^2}{-\Delta P}\right)^{-0.507}\left(\frac{\alpha}{1-\alpha}\right)^{1.823} \qquad (13)$$

The improvements resulting from this modified expression (different exponents and coefficient) are quite apparent in Fig. 11, where the same data have been presented, but using both Eqs. (12) and (13), the latter being employed for non-annular flow conditions.

Examination of the mathematical form of Eqs. (11), (12), and (13) appears to indicate that the correlations are not well-behaved and fail for the limiting cases of $\alpha = 1$ or $\alpha = 0$, i.e., for pure vapor or liquid flows. However, the method of measurement itself fails in these limiting cases also, since for either pure liquid or pure vapor flows the impedance sensed by the probes is constant. Consequently the quantity V_{noise}, generated from the impedance signals, will be zero in these cases and none of the Eqs. (11), (12), and (13) are meaningful. Perhaps the validity of the correlating equations is instead best judged by the

success achieved in predicting v_f and v_g over a range of void fractions up to 0.987 for the data gathered in the SCTF, CCTF, and PKL tests for both steam-water and air-water systems as described herein.

Some comments should be made relative to the significance or importance of constitutive relations in developing the present correlations, specifically the mechanical constitutive relationship involving wall and interfacial shear stress terms. It is not essential to evaluate τ_w or τ_i explicitly in developing the correlations obtained herein rather, it is necessary to evaluate the grouping of terms $\tau_i p_i/A$ and $\tau_w p_w/A$. Both of the preceding groupings of terms, however, can be evaluated from the simplified field Eqs. (9) and (10). Thus, the need for a particular constitutive shear stress relationship, e.g., p. 76, Ref. (13), is not essential for the present purposes.

SUMMARY AND CONCLUSIONS

High-temperature electrical impedance probes have been developed at ORNL for the purpose of making local measurements of two-phase flow parameters in steam-water mixtures. The present paper has focused specifically upon flag type impedance probes designed to make sub-channel, in-core measurements.

The specific objective of the work reported here was to develop analytical and/or empirical algorithms that could be used to calculate the liquid and vapor phase velocities in a variety of two-phase systems, based upon electrical signals from the impedance probes.

Empirical correlations were developed based upon the dimensionless parameters obtained from scaling the governing equations of the two-phase system. The correlations were observed to successfully predict the liquid and vapor phase velocities as would be given by the separated flow model, for both air-water and steam-water systems.

The success of these correlations tends to validate the assumptions utilized in modeling the two-phase flow system. Similarly, the appropriateness and generality of the dimensionless groupings used in the correlations obtained from the simplified field equations appear to have been validated by virtue of a wide variety of data having been correlated from both single and two-component two-phase systems. Results of an error analysis furthermore indicate that the magnitude of the scatter of data associated with the correlations is consistent with propagation of the uncertainties in the measurements of the pertinent system variables.

Finally, from a practical standpoint, the system parameters required in using these correlations are all readily obtainable (measureable) in real operating systems that may employ impedance probes. Specifically, in addition to fluid properties, measurements of void fraction and pressure drop are required, while transit time velocities (V_{noise}) are obtainable from the impedance probe signals by Fast Fourier Transform techniques.

ACKNOWLEDGEMENTS

This research was supported by the Thermal Systems Technology Section of the Engineering Technology Division, Oak Ridge National Laboratory.

REFERENCES

1. J. O. Hylton and R. N. McGill, "Measurement of Velocity and Void Fraction in Steam-Water Mixtures with Electrical Impedance Probes," paper presented at the 3rd CSNI Specialists Meeting on Transient Two-Phase Flow, California Institute of Technology, Pasadena, California, March 23-25, 1981.

2. R. N. McGill, "Phase Velocity Correlations for Impedance Probes in Rod Bundles," paper presented at Review Group Conference on Advanced Instrumentation Research for Reactor Safety, Oak Ridge, Tennessee, July 29-31, 1980.

3. G. Del Tin and A. Negrini, "Development of Electrical Impedance Probes for Void Fraction Measurements in Air-Water Flow," 2nd Multiphase Flow and Heat Transfer Symposium, Miami, Florida, 1978.

4. A. J. Moorhead and C. S. Morgan, "Fabrication of Sensors for High Temperature Steam Instrumentation systems," American Welding Society, 61st Annual Meeting, Los Angeles, California, April 1980.

5. C. S. Morgan, "Thermal Shock Resistant Electrical Insulators," American Ceramic Society, Cincinnati, Ohio, April 1979.

6. W. H. Leavell and J. A. Mullens, "Computation of Transient Phase Interface Velocities in Liquid-Vapor Mixtures, Flow: Its Measurement and Control in Science and Industry," Second International Symposium, St. Louis, Missouri, April 1981.

7. J. E. Hardy and J. O. Hylton, "Electrical Impedance String Probes for Two-Phase Void and Velocity Measurements," NUREG/CR-2505 (ORNL/TM-8172), May 1982.

8. J. G. Collier, "Convective Boiling and Condensation," p. 5, McGraw-Hill, Great Britain, 1972.

9. C. C. Lin and L. A. Segel, "Mathematics Applied to Deterministic Problems in the Natural Sciences," McMillan Publishing Company, 1974.

10. M. Ishii, "Thermo-Fluid Dynamic Theory of Two-phase Flow," Eyrolles, Paris, 1975.

11. C. T. Hsu, Ph.D. Thesis, University of Tennessee, in preparation.

12. G. F. Hewitt and D. N. Roberts, "Studies of Two-Phase Flow Patterns by Simultaneous X-Ray and Flash Photography," AERE-M2159. H.M.S.O., 1969.

13. G. Kocamustafaogullari, "Thermo-Fluid Dynamics of Separated Two-Phase Flow," Ph.D. Thesis, Georgia Institute of Technology, 1971.

14. A. J. Moorman, "TUFASE-Triple-Beam Gamma Densitometer Analytical Model Developed for Two-Phase Flow," Intra-Laboratory Correspondence, BDHT-2130, Oak Ridge National Laboratory, August 1978.

15. K. G. Turnage et. al., "Advanced Two-Phase Flow Instrumentation Program Quarterly progress Report for July-September 1978," ORNL/NUREG/TM-309.

16. G. D. Lassahn, "Loft Three-Beam Densitometer Data Interpretation," Idaho National Engineering Laboratory, Three-NUREG-1111, October 1977.

17. N. C. J. Chen and D. K. Felde, "Modeling of A Turbine Flowmeter in Transient Two-Phase Flow," Proceeding of the 12th Modeling and Simulation Conference, Pittsburgh, Pa., April 1981.

APPENDIX I

UNCERTAINTY ANALYSIS

Additional comments and discussion are warranted relative to (1) uncertainties associated with the experimental data being correlated, and (2) an error analysis of the experimentally based correlations. Before calculating uncertainties of separated flow model equations and correlations, the errors of some of the primary measurements must be estimated first.

Errors in measurements of water flow rates are estimated to be about 0.0126 kg/s (1% full-scale). Steam flow rate errors are estimated to be about 0.0063 kg/s (1% full-scale). Estimated temperature errors are about 1°C, resulting in an error in h_f of about 1 cal/gm and about 0.6 cal/gm in h_g. Pressure measurement errors are estimated to be about 1.72 kPa, resulting in an error of about 2.4 kPa in the pressure drop.

Basically, the gamma densitometer has three beam readings, each of which sense an average density in their paths. A composite density for the two-phase mixture is then calculated by the mathematical models of Ref. (14) and (15), from which the void fraction is then obtained. Lassahn (16) has estimated the error in composite density to be about 0.02 gm/cm³ based upon data from wood/plastic simulations of regular, realistic density distributions. Chen and Felde (17) concluded that the triple-beam gamma densitometer had a 95% confidence level for an error band of 0.067 gm/cm³ for homogeneous flow regimes. The error of 0.067 gm/cm³ reported by Chen and Felde indicates a high percentage error of composite density measurements using a triple-beam gamma densitometer.

In the present study, however, the homogeneous model has been replaced by an annular flow model for calculating void fractions. Consequently, the accuracy should be improved. Again, the 0.02 gm/cm³ error reported by Lassahn tends to give a high percentage error at high void fraction. Nevertheless, the percentage error around the void fraction 0.6-0.9, where most of data points of the present study were obtained, is about 10%. Therefore a percentage error of ±10% in the composite density has been selected for calculation of the void fraction uncertainty herein. Errors in the transit time velocity, V_{noise}, are estimated to be about ±25% by Hardy and Hylton (7).

After estimations of primary measurement errors, the calculations of uncertainties in the separated flow model equations and correlations become possible. For the separated flow model equations, the liquid velocity uncertainty is about 10%, while the vapor velocity has an uncertainty of about 0.6 to 1.2 m/s, which is only a 3% error for high void fraction data (because of the high vapor velocity). However, the percentage error is about ±35% for low void fraction data because of the low vapor velocity.

Table 1 summarizes elements in the uncertainty analysis calculations for the phase velocity correlations. The samples illustrated are selected from a range of void fraction data. The importance and relative magnitudes of the uncertainties in the primary measurements comprising the correlations are evident from the values listed in Table 1. The accumulative effects of these uncertainties are reflected in the estimated uncertainties in the liquid phase velocity and vapor phase velocity. The total estimated error (uncertainty) for the liquid phase velocity is about ±27%, of which the error in the V_{noise} determination accounts for all but 2% of that total (i.e., ±25%). Estimated errors (uncertainties) for the vapor phase velocity are somewhat higher, ranging from 30 to 45%, as would be expected, since the determination of V_g requires the use of previously determined values of V_f from Eq. (11). It is obvious that the accuracy of phase velocity calculations can be improved greatly by reducing the error associated with determining V_{noise}.

Table 1. Summary of Uncertainty Analysis of Phase Velocity Correlations

α	$\frac{\partial V_f}{\partial V_{noise}}(\pm V_{noise})$	$\frac{\partial V_f}{\partial \Delta P}(\pm \Delta P)$	$\frac{\partial V_f}{\partial \alpha}(\pm \alpha)$	$\pm V_f$ (%)	$\frac{\partial V_g}{\partial V_{noise}}(\pm V_{noise})$	$\frac{\partial V_g}{\partial \Delta P}(\pm \Delta P)$	$\frac{\partial V_g}{\partial \alpha}(\pm \alpha)$	$\frac{\partial V_g}{\partial V_f}(\pm V_f)$	$\pm V_g$ (%)
0.724	0.95	0.18	0.35	27	3.32	1.58	3.38	0.96	38
0.743	1.11	0.13	0.4	27	4.33	1.24	4.3	1.06	36
0.77	0.98	0.28	0.34	27	3.89	2.79	3.74	1.10	40
0.787	1.24	0.18	0.42	27	5.17	1.85	4.88	1.13	36
0.812	1.54	0.30	0.51	27	5.89	2.82	5.37	1.03	36
0.83	1.08	0.31	0.35	27	8.36	10.11	5.81	3.61	44
0.845	1.83	0.35	0.57	27	8.81	7.1	5.9	2.2	37
0.886	1.46	0.42	0.44	27	10.35	12.51	6.68	3.28	43
0.908	2.99	0.43	0.89	26	11.18	6.76	7.15	1.68	34
0.942	5.3	0.76	1.58	26	10.47	6.33	6.7	0.89	33
0.967	12.94	1.06	3.96	26	12.45	4.3	8.17	0.43	31
0.987	15.28	1.1	5.38	27	24.65	7.45	18.59	0.73	32